doi:10.1006/jmbi.2001.4529 available online at http://www.idealibrary.com on IDEAL® *J. Mol. Biol.* (2001) **307**, 1023–1034

JMB

Two Divalent Metal Ions in the Active Site of a New Crystal Form of Human Apurinic/Apyrimidinic Endonuclease, Ape1: Implications for the Catalytic Mechanism

Peter T. Beernink, Brent W. Segelke, Masood Z. Hadi, Jan P. Erzberger David M. Wilson III* and Bernhard Rupp*

Molecular and Structural Biology Division, Biology and Biotechnology Research Program, Lawrence Livermore National Laboratory, Livermore CA 94550, USA

*Corresponding authors

The major human abasic endonuclease, Ape1, is an essential DNA repair enzyme that initiates the removal of apurinic/apyrimidinic sites from DNA, excises 3′ replication-blocking moieties, and modulates the DNA binding activity of several transcriptional regulators. We have determined the X-ray structure of the full-length human Ape1 enzyme in two new crystal forms, one at neutral and one at acidic pH. The new structures are generally similar to the previously determined structure of a truncated Ape1 protein, but differ in the conformation of several loop regions and in spans of residues with weak electron density. While only one active-site metal ion is present in the structure determined at low pH, the structure determined from a crystal grown at the pH optimum of Ape1 nuclease activity, pH 7.5, has two metal ions bound 5 Å apart in the active site. Enzyme kinetic data indicate that at least two metal-binding sites are functionally important, since Ca^{2+} exhibits complex stimulatory and inhibitory effects on the Mg^{2+}-dependent catalysis of Ape1, even though Ca^{2+} itself does not serve as a cofactor. In conjunction, the structural and kinetic data suggest that Ape1 catalyzes hydrolysis of the DNA backbone through a two metal ion-mediated mechanism.

Keywords: Ape1 endonuclease; base excision repair; enzyme mechanism; metalloenzyme; abasic DNA

Introduction

Human apurinic/apyridinimic (AP) endonuclease (Ape1) is a multifunctional DNA repair enzyme with 26 % sequence identity to its bacterial homologue, *Escherichia coli* exonuclease III (ExoIII). Like ExoIII, Ape1 functions as an abasic endonuclease in the base excision DNA repair (BER) pathway, hydrolyzing the phosphodiester backbone immediately 5′ to AP sites in DNA.[1] AP sites arise either by spontaneous or damage-induced hydrolysis of the *N*-glycosyl bond or through the repair activity of DNA glycosylases, which remove modified bases as part of BER. Following DNA incision by Ape1, the BER process can proceed through one of several sub-pathways and, in general, involves excision of the 5′-abasic residue remaining after Ape1 cleavage, insertion of a normal nucleotide(s), and ligation of the residual nick (for review, see references[2,3]). Ape1 also exhibits 3′-phosphodiesterase, $3' \rightarrow 5'$ exonuclease and RNase H activities, albeit at far lower efficiencies than its AP endonuclease activity.[4-7] Whereas the physiological roles of the $3' \rightarrow 5'$ exonuclease and RNase H activities are unknown, the 3′-diesterase activity appears to play a role in the processing of 3′-oxidative strand breaks harboring phosphate or phosphoglycolate residues, and other replication blocking

Present address: J. P. Erzberger, Department of Molecular and Cell Biology, University of California, 229 Stanley Hall #3206, Berkeley, CA 94720-3206, USA.

Abbreviations used: AP, apurinic/apyrimidinic; BER, base excision repair; F-DNA, substrate DNA containing a tetrahydrofuran abasic site analog; NCS, non-crystallographic symmetry; NMR, nuclear magnetic resonance; P-DNA, substrate DNA containing a propyl abasic site analogue; rmsd, root-mean-square deviation; rmsf, root-mean-square fluctuation.

E-mail addresses of the corresponding authors: br@llnl.gov; wilson61@llnl.gov

0022-2836/01/041023–12 $35.00/0

moieties.[8-11] All of these nuclease functions are thought to be conferred by a common active site.

A separate function of Ape1, known as its Ref-1 (redox effector factor) activity, is to regulate the DNA-binding affinity of certain transcription factors, such as Jun/Fos and NF-kB, through a reduction/oxidation (redox) mechanism.[12] Ape1 has also been shown to regulate the sequence-specific DNA-binding affinity of p53 through redox-dependent and independent mechanisms.[13] It has therefore been suggested that Ape1 operates as a central component of a signal transduction pathway that regulates the DNA-binding affinity of certain transcription factors in response to environmental stimuli (reviewed in reference[14]). Notably, these regulatory and nuclease functions of Ape1 can be separately inactivated by strategic site-specific or deletion mutagenesis.[15-17]

The crystal structure of a truncated Ape1 protein lacking residues 1-35 has been determined.[18] This structure reveals an α/β-sandwich motif that consists of two six-stranded β-sheets and is structurally similar to the functionally related DNA repair enzyme ExoIII[19] and to the non-specific nuclease DNase I.[20] The active sites of the Ape1 and ExoIII structures each contain one metal ion, which is coordinated predominantly by acidic residues (Asp70 and Glu96 in Ape1). This structural information, in combination with biochemical studies, has been used to gain insight into the molecular mechanisms of the nuclease and regulatory activities of Ape1.

The Ref-1 activity of Ape1 is retained both in an N-terminal fragment comprising residues 1-127[15] and in a C-terminal fragment spanning residues 36 to 318,[21] suggesting that sequences important for Ref-1 function lie between residues 36 and 127. In this span of residues, two cysteines, Cys65 and Cys93, have been implicated as redox cores for modulating the oxidation/reduction state of target transcription factors.[21] However, these amino acid residues appear to occupy buried, inaccessible positions in the Ape1 crystal structure,[18] and thus the precise Ref-1 mechanism remains unclear.

Based on the original crystal structures of Ape1[18] and ExoIII[19] in the absence of DNA, both enzymes were proposed to catalyze phosphodiester bond hydrolysis *via* a single metal ion-assisted reaction. In the proposed reaction scheme, the metal ion presumably functions to orient the scissile phosphate, stabilize the pentacovalent transition-state intermediate and/or polarize the P—O3′ bond. The histidine residue of a ''catalytic triad'' formed by Asp283, His309 and a water molecule in Ape1 (Asp229, His259 and H_2O in ExoIII) acts as a general base to abstract a proton from water, and the resulting hydroxyl ion carries out nucleophilic attack on the phosphorous atom of the DNA backbone 5′ to the abasic site. Consistent with this proposal, mutation of residue His309 to Asn or Ser abolishes Ape1 AP endonuclease activity, while only slightly reducing AP-DNA binding affinity.[6,22-24] Biochemical studies employing site-specific mutants also demonstrated that Asp210 was essential for catalysis.[17,24] Moreover, the finding that replacement of Asp210 by histidine leads to a smaller reduction of Ape1 activity than asparagine or alanine, implied that Asp210 may protonate the leaving group,[24] as previously suggested.[18] This reaction scheme is similar in many respects to the original mechanism of DNase I[25] and *E. coli* RNase H.[26]

Subsequently, three structures of Ape1 complexed with abasic site-containing duplex DNA were determined.[27] The first two structures (1DEW, 1DE8) consisted of Ape1 bound to intact double-stranded AP-DNA in the absence of divalent metal ions, which are important for catalysis. The third structure (1DE9) included Ape1, incised abasic DNA and a Mn ion, which was coordinated both by active-site residues and the abasic-site phosphate. Based on these structures, which represent pre- and post-incision complexes, respectively, an alternative reaction scheme was proposed. In this scheme, Asp210 functions as a general base to generate the nucleophilic hydroxyl ion and His309 acts to orient and polarize the target scissile P—O3′ bond. The single metal ion, coordinated principally by Asp70 and Glu96, plays a role in not only stabilizing the transition-state intermediate, but also in stabilizing the O3′ leaving group.

Notably, each of the crystal forms of Ape1 examined to date have been obtained under conditions of pH that are below the optimal range (pH 6.7-9.0) for its nuclease activity.[28] In an effort to clarify some of the unresolved issues regarding the structure of the N-terminal Ref-1 domain and the specific role of certain amino acid residues in the redox and nuclease reaction mechanisms, we sought to determine the structure of the full-length Ape1 protein under neutral pH conditions. Here we report the structures from two new crystal forms of Ape1, one from neutral and one from acidic pH growth conditions. Our structural data show that Ape1 binds two metal ions in its active site at neutral pH but not at acidic pH, and enzyme kinetics data indicate that two divalent metal ions may be functionally relevant. We discuss the implications of our results on the catalytic mechanism of Ape1 and its structurally conserved homologues. Dynamical information gleaned from our studies also sheds new light on the possible redox mechanism of the mammalian proteins.

Results

pH dependence of Ape1 DNA binding and incision activities

A previous structure of an Ape1 fragment[18] (referred to here as form I) was derived from crystals grown under slightly acidic condtions (pH 6.2), under which little or no Ape1 catalytic activity is observed.[28] We therefore reassessed the optimal pH conditions for both incision activity and the

substrate-specific DNA-binding affinity of Ape1. Within the pH range of 5.0 to 9.6, AP-DNA binding was found to be maximal at or below pH 7.0, with a sharp reduction above pH 7.8 (Figure 1, open circles). DNA incision was optimal between pH 6.6 and 8.6 (Figure 1, filled squares), in good agreement with the previous report.[28] In an effort to characterize the most active form of the enzyme, we optimized crystallization conditions at pH 7.5.

Structure of Ape1 at neutral pH

A new Ape1 crystal form (form III) was obtained at a neutral pH 7.5 (Table 1), in the presence of $Pb(OAc)_2$ and the non-ionic detergent HECAMEG. The form III structure was solved by molecular replacement using the partially refined structure of form II (described below). This form III structure has been determined to 2.2 Å resolution and contains two molecules in the asymmetric unit. The refined model includes 548 out of 636 residues, four Pb ions and 351 water molecules. The N-terminal 42 residues were not visible in the electron density map. In addition, residues 124-125, which comprise a loop region, showed weak electron density and were not modeled. The form III structure has been refined, using tight non-crystallographic symmetry (NCS) restraints, to an R_{cryst} value of 0.186 and an R_{free} value of 0.252 (Table 2).

Structure of Ape1 at acidic pH

Before the neutral pH conditions had been optimized, we obtained a crystal form grown under acidic conditions, referred to as form II (Table 1). The structure was determined to 1.95 Å resolution by molecular replacement, using the form I structure[18] (1BIX) as a search model. The form II structure has one Ape1 molecule per asymmetric unit. The final model includes 257 out of 318 residues, one Pb ion and 292 water molecules, and like form III lacks the N-terminal 43 amino acid residues. The form II structure exhibited weak electron density for residues 102-112 (an α-helix in form I) and 123-127 (a loop in form I), and has been refined to an R_{cryst} value of 0.205 and an R_{free} value of 0.255 (Table 2).

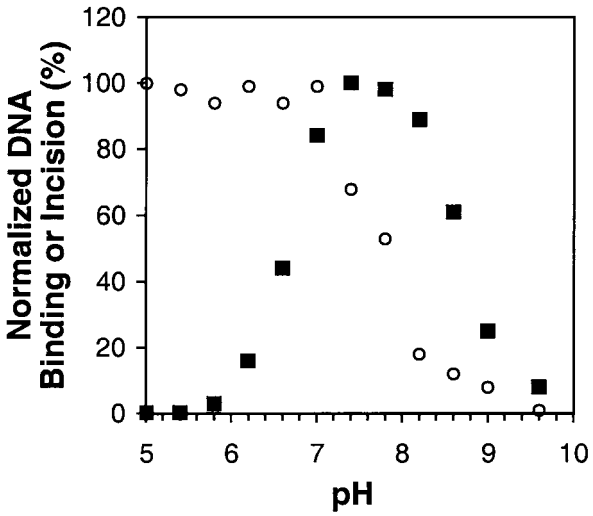

Figure 1. pH profile of Ape1 DNA-binding and nuclease activities. DNA binding (open circles) and incision (filled squares) are plotted as a function of pH. Values were normalized against the maximal value within the pH range tested.

Comparison of Ape1 structures

Crystal forms

The two new crystal forms were grown from solutions of the full-length Ape1 enzyme, whereas the previously determined structure without DNA was obtained from crystals of an Ape1 variant protein with a deletion of 35 N-terminal residues. The crystallization conditions for the three forms differed primarily in the pH at which the crystals were grown and in the metal ion additives (Table 1). The two new crystal forms are in the same space group as the crystal reported previously, *C*2.[18] However, the three crystal forms differ significantly in cell dimensions. Specifically, form II differed from the form I structure in the *a* cell edge, whereas form III differed from form II in the *c* cell edge (Table 1). Form III also differs from the other two in having two molecules in the asymmetric

Table 1. Comparison of Ape1 crystal forms

Crystal form	I[a] (1BIX)	II (1HD7)	III (1E9N)
Protein construct	36-318	1-318	1-318
Crystallization pH	6.2	4.6	7.5
Space group	*C*2	*C*2	*C*2
Cell dimensions (Å)	$a = 87.26$, $b = 44.70$, $c = 78.78$, $\beta = 103.45$	$a = 128.39$, $b = 44.85$, $c = 78.14$, $\beta = 124.54$	$a = 137.52$, $b = 45.02$, $c = 125.70$, $\beta = 108.03$
Molecules/AU[b]	1	1	2
V_M [c] (Å^3/Da)	2.44	2.61	2.61
Metal ions (#/AU[b])	Sm^{3+} (4), Pt^{2+} (1)	Pb^{2+} (1)	Pb^{2+} (4)
Metals ions/active site	1	1	2

[a] Coordinates from reference.[18]
[b] Asymmetric unit of the crystal.
[c] Matthews coefficient.

Table 2. Data processing and refinement statistics

Crystal form (PDB entry)	II (1HD7)	III (1E9N)
Data processing		
Resolution range (Å)	25-1.95	20-2.20
Unique/measured reflections	26,176/91,465	34,905/102,875
Completeness (%)	99.2 (99.3)	93.0 (70.5)
Average $I/\sigma I$	6.1 (1.5)	11.8 (2.1)
R_{sym}[a]	0.074 (0.471)	0.082 (0.379)
Refinement		
R_{cryst}[b]	0.205	0.186
R_{free}[c]	0.255	0.252
rms deviations		
Bond lengths (Å)	0.016	0.018
Bond angles (deg.)	2.0	2.3
Planar groups (Å)	0.030	0.016
NCS internal agreement (Å)[d]	-	0.20

Numbers in parentheses represent data in the highest resolution shell.
[a] $R_{sym} = \Sigma_i(\Sigma_j|I_{ij} - \langle I_i\rangle|)/\Sigma_i\langle I_i\rangle$, for the ith reflection, and the jth observation for each reflection.
[b] $R_{cryst} = \Sigma_i\ ||F_o| - |F_c||/\Sigma|F_o|$, for the ith reflection.
[c] Calculated the same as R_{cryst}, but for 10 % of the data omitted from the refinement.
[d] Non-crystallographic symmetry (NCS) is only present in form III.

unit. The 2-fold NCS provides independent views of variable loop regions and side-chain rotamers and enabled the application of NCS restraints during refinement for large portions of the model.

Disordered or mobile regions

Neither of the Ape1 structures reported here exhibits interpretable density for N-terminal residues 1-42, a region that contains the nuclear localization signals and possibly part of the Ref-1 functional domain. The N-terminal region is also disordered in the recently determined structures of Ape1-DNA complexes, which were obtained using both truncated and full-length Ape1 proteins.[27] In addition, form I lacks electron density for residues 100-104, form II lacks density for 102-112 and 123-127, and form III lacks density for 124-125. The backbone thermal (B) factors, which are highly correlated among the three structures, indicate relatively high thermal motion in the vicinity of residues 100-110, 145, 200 and 270. In agreement with their inferred mobility, these regions also exhibit relatively large root-mean-square fluctuations (rmsf) in molecular dynamics simulations.[29]

Protein conformation

Both of the new structures are substantially similar to the structure of form I (Figure 2). The form II structure superimposes closely with that of form I, exhibiting a root-mean-square deviation (rmsd) of 0.28 Å for backbone atoms (0.88 Å for all atoms) (Figure 2(a) and (b)). While the structures are very similar over most of the polypeptide chain, there are significant (1-2 Å) positional differences bordering the disordered regions (see above) and in the region of Met271 (Figure 2(b), thick, continuous line). These differences are likely attributable to intermolecular crystal contacts, since residues 102-112 are near a symmetry-related molecule in the crystal and Met271 coordinates a lattice-stabilizing Pt ion in the form I structure. The form III structure is slightly more similar to form II (rmsd = 0.29 Å for backbone atoms; 0.86 Å for all atoms) than to form I (rmsd = 0.43 Å for backbone atoms; 0.83 Å for all atoms) (Figure 2). The form III structure also exhibits unique conformations of several loop regions, including residues 105-110 and 120-123 (Figure 2(b)). Moreover, the three unliganded Ape1 structures exhibit ~2 Å backbone differences around residues 100, 110 and 125 relative to the structures of Ape1-DNA complexes.[25] Each of these three regions is disordered in at least one of the free Ape1 structures, indicating that the DNA recognition loops are mobile in the absence of DNA.

Metal sites

The most striking difference among the three crystal forms was the number and location of metal ions present in the structures (Table 1). The intermolecular contact regions of form I contain four heavy metal ions (three Sm^{3+} and one Pt^{2+}), which are not present in the form II or form III structures. The low pH structures, forms I and II, contain a Sm^{3+} and a Pb^{2+} in the active site, respectively. In stark contrast, two Pb ions are observed the active site of the neutral pH structure, form III (Figure 3). One of the Pb ions in the active site of form III superimposes closely on the Pb^{2+} in form II and the Sm^{3+} in form I. We refer to this originally observed metal-binding site as site A. In all three structures, the metal in site A (metal A) is coordinated by the carboxylates of residues Asp70 and Glu96. In forms II and III, metal A also coordinates a water molecule, which forms hydrogen bonds with both Asn68 and Asp308.

The second metal binding site (site B) in form III is composed of the side-chains of Asp210, Asn212 and His309. The two metal ions are 5.0 Å apart

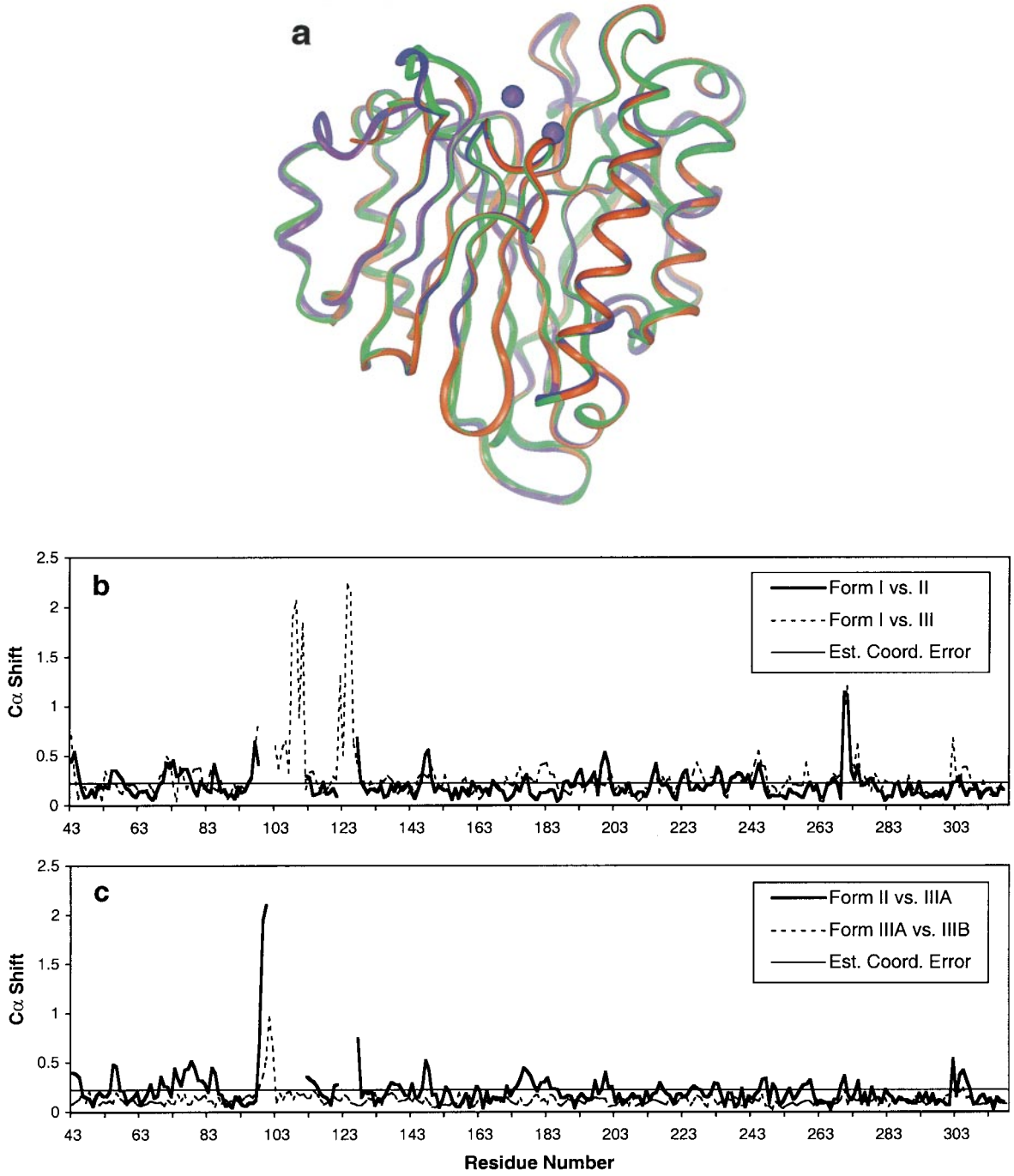

Figure 2. Superposition of Ape1 structures. (a) Ribbon representation of the backbone atoms of the three crystal forms are shown (form I, green; form II, red; form III, violet). Conformational differences are seen in regions positioned near the top left region of the panel. The two metal ions in the form III structure are depicted as purple spheres. Structures were superimposed using GEM[30] and the image was generated with InsightII (Molecular Simulations, Inc.). (b) Differences in C^{α} positions (Å) plotted *versus* residue number. Comparisons to form I are shown. The thin, continuous line represents the coordinate error estimated from the R_{free} value[31] in the refinement of form III. (c) Similar comparisons involving form III are shown. IIIA and IIIB refer to the two molecules of the form III structure that are related by NCS.

and the metal ion at site B also coordinates a water molecule that contacts Tyr171 (Figure 3). There is no carboxylate group bridging the two metal ions, as has been seen in many bimetallic enzymes.[34-36] However, an indirect bridge is formed by Asn68, which forms hydrogen bonds with the carboxylates of Glu96 and Asp210, each of which interacts with one of the metal ions (Figure 3). The metal-coordinating residues are in very similar positions in all known Ape1 structures, which indicates that

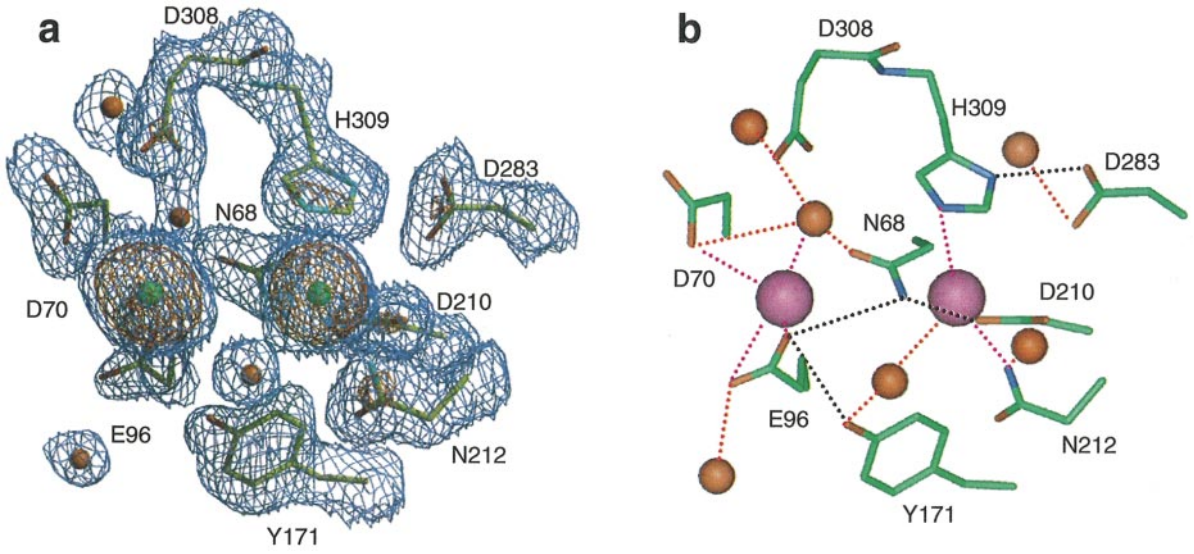

Figure 3. Active site region of human Ape1 crystal form III. (a) wARP electron density map (see Materials and Methods) showing the two Pb ions (green spheres) bound at the active site. The map is shown at contour levels of 1.5σ (blue) and 5σ (red). The image was generated with XtalView[32] and Raster3D.[33] (b) Stick rendering of the same region, showing electrostatic interactions. The two Pb ions are shown as pink spheres and water molecules are shown as red spheres. The interactions (non-hydrogen atoms <3.3 Å apart) are depicted as dotted lines; metal interactions (magenta), water interactions (red) and protein interactions (black) are shown. The image was generated with InsightII (BIOSYM/Molecular Simulations, Inc., San Diego, CA).

site A is not significantly affected by the specific metal that is bound (Mn^{2+}, Sm^{3+} or Pb^{2+}). Similarly, the side-chains in site B are in virtually identical positions, suggesting that this binding site is preformed in the absence of metal ions.

Functional evidence for two metal binding sites

Assays in the presence of one productive and one non-productive metal have been used to distinguish between one and two metal ion involvement in catalysis.[37] For an enzyme that has two metal-binding sites, each with a distinct binding affinity, titration with a non-productive metal should yield biphasic inhibition curves or stimulation of activity followed by inhibition. *Eco*RV, which is a presumed two-metal utilizing endonuclease, exhibited the latter effects when Ca^{2+} was titrated in the presence of a fixed concentration of Mg^{2+}.[37] Presumably, these effects arise because the ''non-productive'' metal, Ca^{2+}, can substitute functionally at one site, but not at the other.

Similar experiments with Ape1 were performed to examine whether a second metal may be involved in its activity. Ape1 can utilize Mg^{2+} or Mn^{2+} as a cofactor in catalysis,[6,28] but has extremely low specific activity (<0.02% of the 10 mM Mg^{2+} level) in the presence of EDTA, which chelates any available Mg^{2+}.[24] No increase in Ape1 specific activity, relative to that in the presence of EDTA, was detected in the presence of 0.1-10.0 mM Ca^{2+} (data not shown). Therefore, we assessed, sites by varying the ratio of Ca^{2+} to Mg^{2+}, whether titration of non-productive Ca ions had an effect on Ape1 activity that was characteristic of two functionally relevant metal-binding. At higher Ca^{2+}/Mg^{2+} ratios (i.e. 0-3 mM Mg^{2+}), Ca^{2+} led to stimulation of activity relative to the Mg^{2+} alone controls (Figure 4(a)). In contrast, at lower Ca^{2+}/Mg^{2+} ratios (i.e. 3-10 mM Mg^{2+}), Ca^{2+} was inhibitory relative to Mg^{2+} alone. These bimodal effects and particularly the significant stimulation of activity by non-productive Ca ions (Figure 4(b)) provide functional evidence that a second metal ion may be involved in Ape1 catalysis.

Discussion

Ape1 conformational dynamics

The loop regions of Ape1 consisting of residues 100-110 and 120-125 exhibit significant structural variation, displaying >2 Å backbone differences among the three structures (Figure 2). These conformational differences may arise from crystal packing interactions or differences in the pH of crystallization, but are likely not the result of the additional bound metal in form III, since the mobile regions are generally distant from binding site B. Interestingly, despite the significant backbone differences noted above, the three active-site conformations are very similar, consistent with the notion that Ape1 maintains a relatively rigid binding and catalytic pocket.[27] It remains to be determined whether the structural flexibility of Ape1 has a functional role, such as in the coordination of BER, potentially through direct protein-protein interactions.

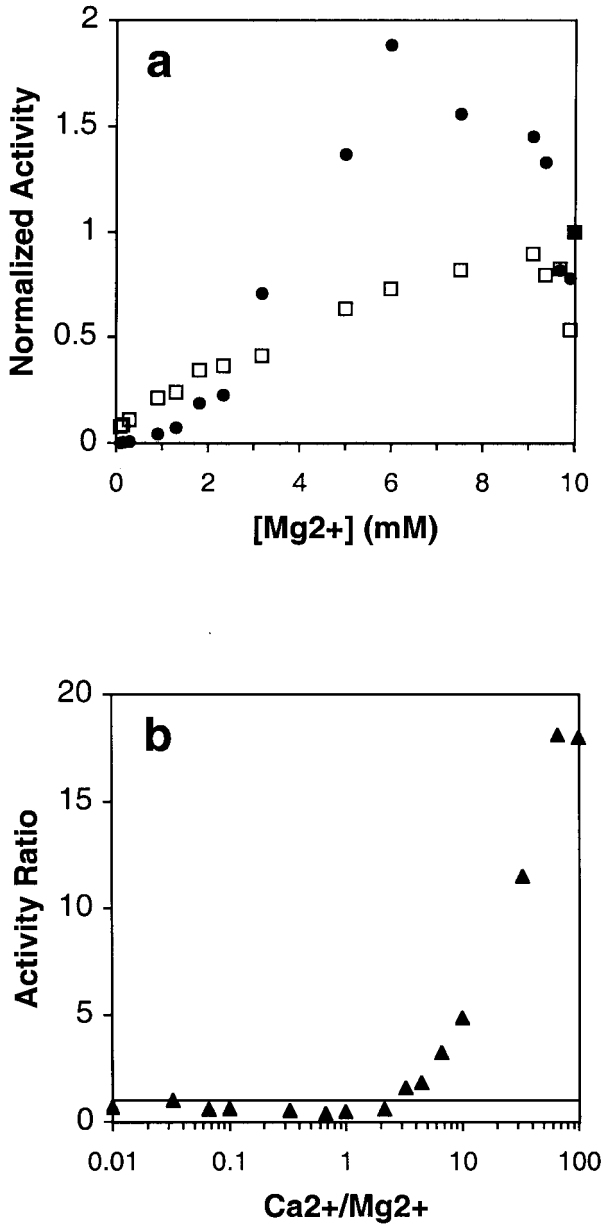

Figure 4. Ape1 incision assays in the presence of mixed metals. DNA hydrolysis was assayed in the presence of varying concentrations of Mg^{2+}, in the absence or presence of Ca^{2+}. In the mixed metal reactions, the total metal concentration was 10 mM. The specific activities were normalized to the level in the presence of 10 mM Mg^{2+}. (a) Normalized activity *versus* [Mg^{2+}] for reactions lacking (filled circles) or containing Ca^{2+} (open squares). (b) Semi-logarithmic plot of the same data as in (a) plotted as normalized activity ratio $((Ca^{2+} + Mg^{2+})/Mg^{2+})$ *versus* the Ca^{2+}/Mg^{2+} ratio. Note that data points in (b) are inverted on the abscissa relative to (a). A line representing $y = 1$ is shown to distinguish activation ($y > 1$) from inhibition ($y < 1$).

The redox regulatory domain

Thioredoxin is a known regulator of the redox state of Ape1 *in vivo*.[38] In an NMR structure of thioredoxin bound to a peptide corresponding to residues 58-71 of Ape1, Cys32 of thioredoxin forms a disulfide bridge with Cys65 of the Ape1 peptide.[39] The details of the Ape1 redox function have nevertheless remained obscure, primarily since the presumed regulatory residue Cys65 appears buried in the unliganded Ape1 structure by Gorman *et al*.[18] Thus, in the context of the full-length Ape1 protein, redox-specific interactions would need to occur to expose Cys65. This event could be accomplished by rotation of the side-chain of Tyr83, or a larger reorientation of the loop containing residues 80-85. Evidence for mobility in this region is provided by higher-than-average rms fluctuations in molecular dynamics simulations[29] and crystallographic temperature (*B*) factors in all three unliganded Ape1 structures (1BIX (18), 1E9N and 1HD7 (this work)). It is also noteworthy that the redox active residue of thioredoxin, Cys32, is located on a protrusion of the protein, which could facilitate interaction with an amino acid in a partially buried position.[39] Since residues Asn68 and Asp70 have been implicated in the nuclease activity of Ape1, it is unlikely that it remains active as a nuclease when bound to thioredoxin. As in the form I structure,[18] forms II and III exhibit an intermolecular disulfide bond between NCS-related Cys138 residues. Whereas no biological role for Ape1 oligomerization has been proposed, dimerization could alter the ability of Ape1 to interact with thioredoxin, other proteins or DNA, and thereby act as a mechanism of regulating some or all of its functions *in vivo*.

A newly proposed catalytic mechanism for Ape1

While the previous catalytic mechanisms cannot be ruled out, based on the form III crystal structure, which contains two active-site divalent metal ions, and the complex effects of metals observed here, we propose that Ape1 executes a two metal-assisted reaction (Figure 5(a)). The observation of a metal ion bound at site B under neutral (pH 7.5), but not acidic conditions (pH 4.6-6.2), suggests that deprotonation of a residue in this site may allow metal binding. Furthermore, this ionization may be manifested in the acidic limb of the pH profile, which implicates in catalysis an ionizible group with a pK_a value of ~6.6, consistent with an unperturbed His residue (e.g. His309). Since all of the important catalytic residues have a role in coordinating a metal ion (Figure 3), the most likely candidate to deprotonate a water molecule (or stabilize a hydroxyl ion) and generate the required catalytic nucleophile is a Mg ion. This is plausible, since metal-bound hydroxyl ions are potent nucleophiles and promote reactions whose rates are not especially sensitive to the pK_a value of the bound water molecule.[41]

Based on a superposition of the form III structure and the Ape1-DNA complex structure,[27] the positions of the two metal ions relative to DNA

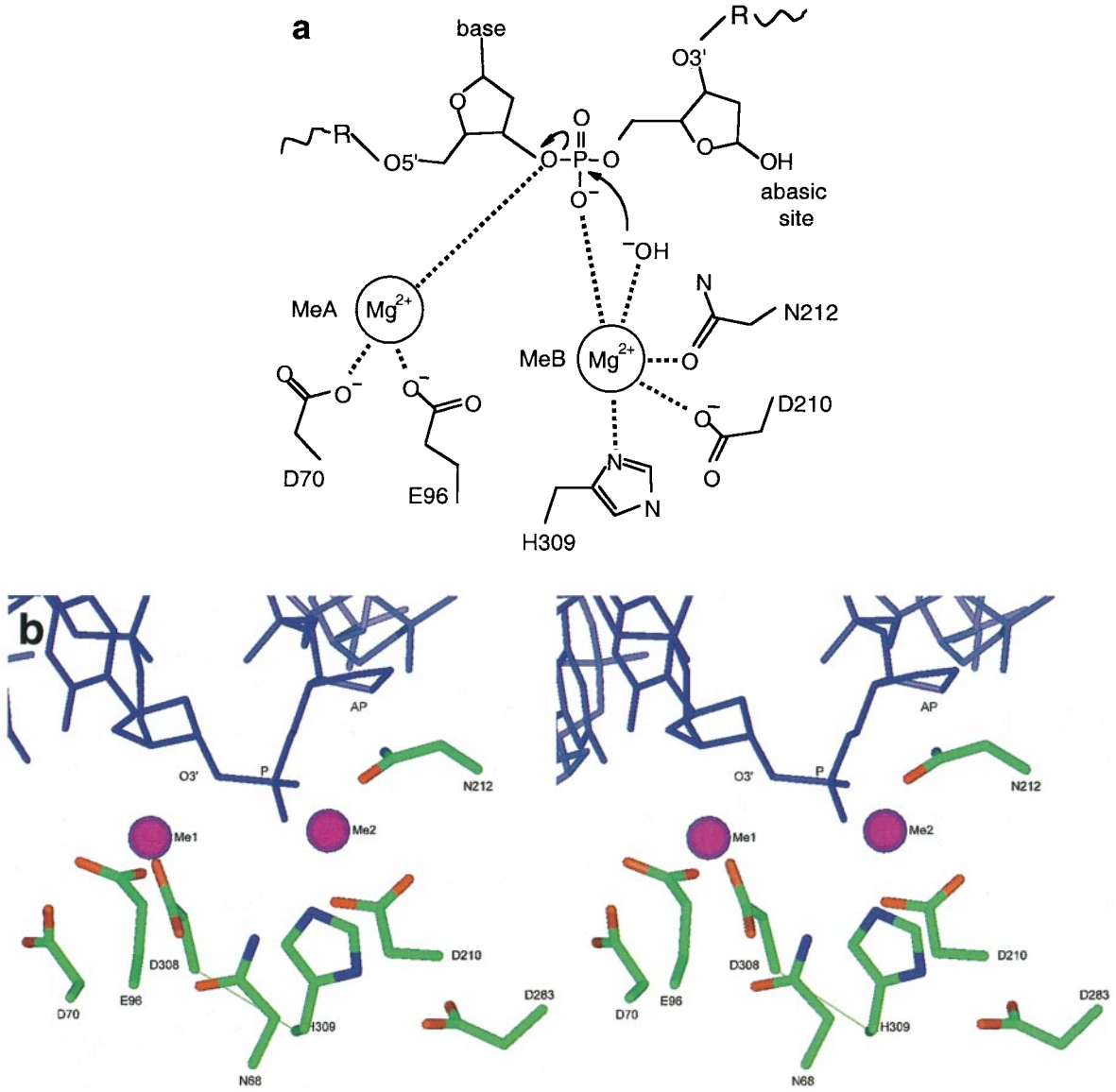

Figure 5. Proposed catalytic mechanism for Ape1 hydrolysis of DNA. (a) A portion of the DNA backbone is shown at the top, with the abasic residue shown on the 5′ (right) side. The continuation of the DNA backbone is represented by R groups and wavy lines. The primary residues coordinating the two metal ions are shown, with site A (Asp70 and Glu96) on the left and site B (Asp210, Asn212 and His309) on the right. In the proposed mechanism, the Mg^{2+} in site A coordinates an hydroxyl ion, which carries out nucleophilic attack on the phosphorous 5′ to the abasic nucleotide. The Mg^{2+} in site B acts to neutralize the charge of the pentacovalent intermediate and/or stabilize the 3′ leaving group. Asn212 and His309 also interact with DNA (interactions not shown) and these residues, when substituted have approximately 10^4-fold[40] and 13-fold[23] reductions in DNA-binding affinity, respectively. (b) Model of an Ape1-metal-DNA complex. A stereo image of a modeled complex of Ape1, bound metal ions and abasic DNA is shown. Selected Ape1 side-chains (colored by atom) and the associated metal ions (pink) are from the form III structure and the DNA (blue) is from PDB entry 1DEW.[27] The protein structures were superimposed using the backbone atoms of residues 43-318 using GEM[30] and the Figure was generated using InsightII (BIOSYM/Molecular Simulations, Inc., San Diego, CA). The positions of the scissile bond (P—O3′) and the abasic sugar ring (AP) are indicated.

can be inferred (Figure 5(b)). This model is likely to represent the pre-active complex, since the active-site residues are in very similar positions in all known Ape1 structures, regardless of the presence of metal ions or DNA. In the modeled complex, the metal at site B (composed of residues Asp210, Asn212 and His309) is juxtaposed next to O1P and O2P, the two non-esterified oxygen atoms of the scissile phosphate†. Since metal B is closer to the scissile phosphate, it likely stabilizes the hydroxyl ion that is proposed to act as the nucleo-

† In the modeled complex, Me2 is 1.4 Å from O1P and 2.4 Å from O2P. These distances may be slightly different in the hypothesized Ape1-DNA-$2Mg^{2+}$ complex.

phile. Metal B is also in a favorable position to neutralize the negative charge of the phosphorane transition-state intermediate. The model places the metal at site A (composed of Asp70 and Glu96) 2.7 Å from the O3′ atom that is 5′ to the abasic ribose. Metal A is in a favorable position to stabilize the 3′ leaving group, as previously proposed.[18,27] In addition, metal A, which is 3.9 Å from O1P (or O2P), can potentially interact with another phosphate oxygen atom on formation of the trigonal bipyramidal transition-state intermediate. This catalytic reaction scheme bears close similarity to the two-metal mechanism that was proposed for the exonuclease domain of *E. coli* DNA polymerase I,[34] since the metal ions are in similar positions relative to the phosphate groups in the two structures.

Further evidence for a two-metal mechanism

Other lines of evidence suggest that two metals may be involved in Ape1 catalysis as well. First, a sigmoidal dependence of enzyme activity on Mg ion concentration has been observed at low Mg^{2+} concentrations,[42] a phenomenon that is characteristic of a two-metal mechanism.[43] Second, two apparently distinct roles for the metal ion(s) in the Ape1 incision reaction have been identified, one in catalysis and one in product release, as determined by single-turnover and steady-state enzyme kinetics.[42] Importantly, the two-metal mechanism also explains the essential role for both Asp210 and His309 in catalysis, as each residue constitutes part of metal site B (Figure 3). In addition, our proposal accounts for the less dramatic reductions in activity caused by mutations of other residues in the Ape1 active site (Figure 3), including Asn68 (200 to 600-fold; L. Nguyen & D.M.W. III, unpublished results), Tyr171 (>fivefold),[24] Asp283 (10 to 30-fold)[22,23] and Asp308 (fivefold),[6,22,24] all of which interact indirectly with a metal ion.

A noteworthy correlation exists between substitutions at each of the two metal binding sites and their effects on catalysis. Specifically, mutagenesis of Asp70 or Glu96 in metal-binding site A of Ape1 has a relatively moderate effect on catalysis, with reductions in specific activity of 25 or 600-fold, respectively.[6,24] In contrast, substitution of residues Asp210, Asn212 or His309 at site B has a more severe effect on catalysis, with a $>10^4$-fold reduction in activity.[22-24,40] Thus, site B appears to play a more important role than site A, based on the effects of mutagenesis. However, it is possible that site A of Ape1 can bind a metal ion in the absence of one of its two protein ligands. In support of this proposal, neither ExoIII nor DNase I has an acidic residue at the position corresponding to Asp70 of Ape1, yet each binds a metal ion at the corresponding position. Alternatively, it is possible that the metal A can be functionally substituted, albeit inefficiently, for example, by a monovalent cation or a water molecule.

It is somewhat perplexing that a low residual activity was detected for wild-type Ape1 on a tetrahydrofuran abasic site analogue substrate (F-DNA) in the presence of 4 mM EDTA (~0.01 % of the level in 10 mM Mg^{2+}).[22,24] Furthermore, a propane abasic site analogue (P-DNA), which lacks the ribose ring structure and displays increased DNA backbone flexibility,[44] was incised at a substantial rate in the absence of divalent metal ions (3 % of the 10 mM Mg^{2+} level;[24]). As previously discussed, it is not likely that Ape1 has tightly bound divalent metal ions[6,45] or that the DNA substrates used were contaminated with metals.[24] Thus, in face of a two-metal mechanism, these observations suggest that, first, the major role of the metal ions in hydrolysis is to stabilize a specific DNA conformation that allows nucleophilic attack, particularly on ring-containing abasic substrates, and second, that generation of the active-site nucleophile and stabilization of the leaving group can proceed through an alternative, divalent metal-independent, mechanism. The residual incision activity observed with F-DNA and the substantial cleavage of P-DNA in the absence of divalent metal ions can be explained if monovalent cations or water molecules permit catalysis at some low level, particularly in the context of increased DNA backbone mobility, as observed with acyclic AP sites.

Implications for exonuclease III structural homologues

The structurally conserved family of endonucleases, which includes Ape1, ExoIII and DNase I, is likely to carry out phosphodiester bond hydrolysis by a common mechanism. This family has been thought to utilize a one metal-ion mechanism, based on the presence of a single metal ion in all three crystal structures. However, in these earlier studies, each of the enzymes was crystallized under acidic conditions ($\leqslant$pH 6.2). Several independent lines of biochemical evidence have since suggested that these proteins, which use the metal ion for several different aspects of catalysis, may employ two metals in the reaction scheme. For example, although one divalent metal ion is observed in the active site of the DNase I structure,[20] the results of site-specific mutagenesis, together with geometric and electrostatic considerations, suggested that residue Asp168 comprised a second metal-binding site.[46] Our structural evidence indicates that the corresponding residue, Asp210, in the structurally similar enzyme Ape1, constitutes part of metal site B. In addition, ExoIII was observed to bind two Mn ions, but only one Mg ion, by isothermal titration calorimetry.[47] These experiments suggest that ExoIII may act through a two-metal mechanism and demonstrate the non-equivalent binding affinities of the two sites for different metal ions. In light of the considerable activation of Mg^{2+}-dependent Ape1 activity by Ca^{2+}, it is possible that Ape1 uses two different metals *in vivo*, as suggested for the exonuclease domain of DNA polymerase I.[34] Thus, for Ape1,

ExoIII and DNase I, complementary pieces of evidence suggest that each enzyme acts through a two-metal catalytic mechanism. These hypotheses warrant further biochemical experiments and structure determinations to establish unequivocally the catalytic mechanism of this family of biologically important endonucleases.

Materials and Methods

Protein purification and crystallization

Human Ape1 was purified from *E. coli* BL21(DE3) as described.[24] Crystals were grown at 4 °C by vapor diffusion in hanging drops from 10-12 mg/ml protein solutions. Hanging drops (6 μl) consisted of equal volumes of protein and well solutions. The well solution for form II was 0.1 M sodium acetate (pH 4.6), 25 % (w/v) polyethylene glycol 4000, 1 mM lead (II) acetate and for form III was 0.1 M Tris-HCl (pH 7.5), 0.2 M sodium acetate, 25 % polyethylene glycol 4000, 1 mM lead (II) acetate and 19.5 mM HECAMEG (Hampton Research, Inc., Laguna Niguel, CA). Using conditions similar to those used to obtain form III crystals, a metal screen was performed, which yielded crystals only in the presence of $Sm(OAc)_2$ or $Pb(OAc)_2$ ($Mg(OAc)_2$, $MnCl_2$ and $NiCl_2$ were also tested). For both forms, monoclinic crystals (ca. 0.1 mm× 0.3 mm × 1.0 mm) were obtained in several weeks.

Data collection, structure refinement and analysis

The low pH crystal (form II) diffraction data were collected from a single crystal at beam line 5.0.2 at the Advanced Light Source, Lawrence Berkeley National Laboratory. Neutral pH crystal (form III) diffraction data were collected from a single crystal at beam line 1-5 at the Stanford Synchrotron Radiation Laboratory. Data were reduced with MOSFLM[48] and SCALA.[49] Molecular replacement was done with EPMR,[50] using the form I structure[18] (1BIX) as a search model to solve form II and the partially refined form II structure to solve form III.

Electron density maps were calculated using a modification[51] of the wARP procedure,[52] consisting of six independent runs of unrestrained refinement starting with perturbed dummy models. Refinement of the structures was performed with REFMAC[31] and TNT.[53] For form III, which contained two molecules in the asymmetric unit, tight non-crystallographic symmetry restraints were imposed and were relaxed at the end of refinement. The solvent structure was built with Arp/Warp 5.0[54] and manual rebuilding was carried out with XtalView.[32] Structure validation was performed with PROCHECK[49] and WHAT CHECK.[55]

DNA binding and incision assays

DNA binding and AP endonuclease assays were performed using radiolabeled 18 base-pair duplex DNA substrates, with one strand containing a tetrahydrofuran (F) abasic site analog. pH titration experiments were conducted at a constant ionic strength using a multiple buffer system,[46] consisting of 50 mM (of each component) acetic acid/MES/HEPES/TAPS/CAPSO, adjusted to pH values between 5.0 and 9.6 in 0.2 unit increments with NaOH. For DNA-binding measurements, 0.05 % (v/v) Triton X-100 and 50 mM KCl were also present. DNA-binding reactions were incubated under various pH conditions on ice and the products were separated on a non-denaturing polyacrylamide gel at neutral pH.[24] Nuclease assays included the aforementioned buffer system, 0.05 % Triton X-100, 50 mM KCl and 10 mM $MgCl_2$, unless otherwise noted. Radiolabeled DNA was visualized and quantified using a STORM 860 Phosphorimager (Molecular Dynamics, Inc., Sunnyvale, CA) and the associated ImageQuant v2.10 software package. DNA-binding data are given as the percent in complex with protein and DNA incision data as the percent of DNA converted to product.

Metal titrations of AP endonuclease activity were performed under standard assay conditions,[24] except that the amounts of $MgCl_2$ and $CaCl_2$ were varied (see the legend to Figure 4). The combined divalent metal ion concentration was 10 mM in the mixed metal reactions. No increase in Ape1 specific activity relative to EDTA containing control reactions was obtained with either 0.1-10 mM $CaCl_2$†. Visualization and quantification of substrates and products were carried out as above. Specific activity values were normalized against the level obtained in 10 mM $MgCl_2$. The error is estimated to be ±10%.

Data Bank accession numbers

Atomic coordinates and structure factor amplitudes have been deposited in the RCSB Protein Data Bank. The accession number for the acidic pH structure (form II) is 1HD7 and that for the neutral pH structure (form III) is 1E9N.

† It is worth noting that Ape1 exhibited <1 % of normal activity in buffers containing 0.1, 1.0 or 10 mM $Pb(OAc)_2$. For various technical reasons, it is not uncommon to find discrepancies between metals in crystal structures and metals used in *in vitro* enzyme activity assays (reviewed in reference[43]).

Acknowledgments

We gratefully thank Mark Knapp (LLNL) for data collection. X-ray diffraction data were collected at Stanford Synchrotron Radiation Laboratory Beam Line 1-5 and the Advanced Light Source Beam Line 5.0.2. Sabine Ringhofer and Michael Forstner (LLNL) participated in the early stages of model building and structure refinement. SSRL is operated by the Department of Energy, Office of Basic Energy Sciences. ALS is supported by the Director, Office of Science, Office of Basic Energy Sciences, Materials Sciences Division, of the US Department of Energy under contract number DE-AC03-76SF00098 at Lawrence Berkeley National Laboratory. This work was carried out under the auspices of the US Department of Energy by Lawrence Livermore National Laboratory under contract number W-7405-ENG-48 and was in part supported by NIH grant CA79056 (to D.M.W. III).

References

1. Demple, B. & Harrison, L. (1994). Repair of oxidative damage to DNA: enzymology and biology. *Annu. Rev. Biochem.* **63**, 915-948.

2. Wilson, S. H. (1998). Mammalian base excision repair and DNA polymerase beta. *Mutat. Res.* **407**, 203-215.
3. Lindahl, T. (2000). Suppression of spontaneous mutagenesis in human cells by DNA base excision-repair. *Mutat. Res.* **462,**, 129-135.
4. Chen, D. S., Herman, T. & Demple, B. (1991). Two distinct human DNA diesterases that hydrolyze 3′-blocking deoxyribose fragments from oxidized DNA. *Nucl. Acids Res.* **19**, 5907-5914.
5. Wilson, D. M., III, Takeshita, M., Grollman, A. P. & Demple, B. (1995). Incision activity of human apurinic endonuclease (Ape) at abasic site analogs in DNA. *J. Biol. Chem.* **270**, 16002-16007.
6. Barzilay, G., Mol, C. D., Robson, C. N., Walker, L. J., Cunningham, R. P., Tainer, J. A. & Hickson, I. D. (1995). Identification of critical active-site residues in the multifunctional human DNA repair enzyme HAP1. *Nature Struct. Biol.* **2**, 561-568.
7. Barzilay, G., Walker, L. J., Robson, C. N. & Hickson, I. D. (1995). Site-directed mutagenesis of the human DNA repair enzyme HAP1: identification of residues important for AP endonuclease and RNase H activity. *Nucl. Acids Res.* **23**, 1544-1550.
8. Winters, T. A., Henner, W. D., Russell, P. S., McCullough, A. & Jorgensen, T. J. (1994). Removal of 3′-phosphoglycolate from DNA strand-break damage in an oligonucleotide substrate by recombinant human apurinic/apyrimidinic endonuclease 1. *Nucl. Acids Res.* **22**, 1866-1873.
9. Suh, D., Wilson, D. M., III & Povirk, L. F. (1997). 3′-phosphodiesterase activity of human apurinic/apyrimidinic endonuclease at DNA double-strand break ends. *Nucl. Acids Res.* **25**, 2495-2500.
10. Izumi, T., Hazra, T. K., Boldogh, I., Tomkinson, A. E., Park, M. S., Ikeda, S. & Mitra, S. (2000). Requirement of human AP endonuclease 1 for repair of 3′-blocking damage at DNA single-strand breaks induced by reaction oxygen species. *Carcinogenesis,* **21**, 1329-1334.
11. Chou, K.-M., Kukhanova, M. & Cheng, Y.-C. (2000). A novel action of human apurinic/apyrimidinimic endonnuclease. Excision of L-configuration deoxyribonucleoside analogs from the 3′ termini of DNA. *J. Biol. Chem.* **275**, 31009-31015.
12. Xanthoudakis, S., Miao, G., Wang, F., Pan, Y.-C. E. & Curran, T. (1992). Redox activation of Fos-Jun DNA binding activity is mediated by a DNA repair enzyme. *EMBO J.* **11**, 3323-3335.
13. Jayaraman, L., Murthy, K. G., Zhu, C., Curran, T., Xanthoudakis, S. & Prives, C. (1997). Identification of redox/repair protein Ref-1 as a potent activator of p53. *Genes Dev.* **11**, 558-570.
14. Evans, A. R., Limp-Foster, M. & Kelley, M. R. (2000). Going Ape over Ref-1. *Mutat. Res.* **461**, 83-108.
15. Xanthoudakis, S., Miao, G. & Curran, T. (1994). The redox and DNA-repair activities of Ref-1 are encoded by nonoverlapping domains. *Proc. Natl Acad. Sci. USA,* **91**, 23-27.
16. Izumi, T. & Mitra, S. (1998). Deletion analysis of human AP-endonuclease: minimum sequence required for the endonuclease activity. *Carcinogenesis,* **19**, 525-527.
17. Rothwell, D. G., Hang, B., Gorman, M. A., Freemont, P. S., Singer, B. & Hickson, I. D. (2000). Substitution of Asp-210 in HAP1 (APE/Ref-1) eliminates endonuclease activity but stabilizes substrate binding. *Nucl. Acids Res.* **28**, 2207-2213.
18. Gorman, M. A., Morera, S., Rothwell, D. G., de La Fortelle, E., Mol, C. D. & Tainer, J. A. *et al.* (1997). The crystal structure of the human DNA repair endonuclease HAP1 suggests the recognition of extra-helical deoxyribose at DNA abasic sites. *EMBO J.* **16**, 6548-6558.
19. Mol, C. D., Kuo, C.-F., Thayer, M. M., Cunningham, R. P. & Tainer, J. A. (1995). Structure and function of the multifunctional DNA-repair enzyme exonuclease III. *Nature,* **374**, 381-386.
20. Suck, D., Oefner, C. & Kabsch, W. (1984). Three dimensional structure of bovine pancreatic DNase I at 2.5 Å resolution. *EMBO J.* **3**, 2423-2430.
21. Walker, L. J., Robson, C. N., Black, E., Gillespie, D. & Hickson, I. D. (1993). Identification of residues in the human DNA repair enzyme HAP1 (Ref-1) that are essential for redox regulation of Jun DNA binding. *Mol. Cell Biol.* **13**, 5370-5376.
22. Masuda, Y., Bennett, R. A. O. & Demple, B. (1998). Rapid dissociation of human apurinic endonuclease (Ape1) from incised DNA induced by magnesium. *J. Biol. Chem.* **273**, 30360-30365.
23. Lucas, J. A., Masuda, Y., Bennett, R. A. O., Strauss, N. S. & Strauss, P. R. (1999). Single turnover analysis of mutant human apurinic/apyrinidimic endonuclease. *Biochemistry,* **38**, 4958-4964.
24. Erzberger, J. P. & Wilson, D. M., III (1999). The role of Mg^{2+} and specific amino acid residues in the catalytic reaction of the major human abasic endonuclease: new insights from EDTA-resistant incision of acyclic abasic site analogs and site-directed mutagenesis. *J. Mol. Biol.* **290**, 447-457.
25. Weston, S. A., Lahm, A. & Suck, D. (1992). X-ray structure of the DNase I-d$(GGTATACC)_2$ complex at 2.3 Å resolution. *J. Mol. Biol.* **226**, 1237-1256.
26. Nakamura, H., Oda, Y., Iwai, S., Inoue, H., Ohtsuka, E. & Kanaya, S. *et al.* (1991). How does RNase H recognize a DNA. RNA hybrid? *Proc. Natl Acad. Sci. USA,* **88**, 11535-11539.
27. Mol., C. D., Izumi, T., Mitra, S. & Tainer, J. A. (2000). DNA bound structures and mutants reveal abasic DNA binding by APE1 DNA repair and coordination. *Nature,* **403**, 451-455.
28. Kane, C. M. & Linn, S. (1981). Purification and characterization of an apurinic/apyrimidinic endonuclease from HeLa cells. *J. Biol. Chem.* **256**, 3405-3414.
29. Nguyen, L. H., Barsky, D., Erzberger, J. P. & Wilson, D. M., III (2000). Mapping the protein-DNA interface and the metal-binding site of the major human apurinic/apyrinidimic endonuclease. *J. Mol. Biol.* **298**, 447-459.
30. Fauman, E. B., Rutenber, E. E., Maley, G. F., Maley, F. & Stroud, R. M. (1994). Water-mediated substrate/product discrimination: the product complex of thymidylate synthase at 1.83 Å. *Biochemistry,* **33**, 1502-1511.
31. Murshudov, G., Vagin, A. & Dodson, E. (1997). Refinement of macromolecular structures by the maximum-liklihood method. *Acta Crystallog. sect. D,* **53**, 240-255.
32. McRee, D. E. (1992). XtalView: a visual protein crystallographic software system for X11/XView. *J. Mol. Graph.* **10**, 44-47.
33. Merritt, E. A. & Bacon, D. J. (1997). Raster3D: Photorealistic molecular graphics. *Methods Enzymol.* **277**, 505-524.
34. Beese, L. S. & Steitz, T. A. (1991). Structural basis for the 3′-5′ exonuclease activity of *Escherichia coli*

DNA polymerase I: a two metal ion mechanism. *EMBO J.* **10**, 25-33.
35. Horton, J. R. & Cheng, X. (2000). *Pvu*II endonuclease contains two calcium ions in active sites. *J. Mol. Biol.* **300**, 1049-1056.
36. Doublié, S., Tabor, S., Long, A. M., Richardson, C. C. & Ellenberger, T. (1998). Crystal structure of a bacteriophage T7 DNA replication complex at 2.2 Å resolution. *Nature,* **391**, 251-258.
37. Vipond, I. B., Baldwin, G. S. & Halford, S. E. (1995). Divalent metal ions at the active sites of the *Eco*RV and *Eco*RI restriction endonucleases. *Biochemistry,* **34**, 697-704.
38. Hirota, K., Matsui, M., Iwata, S., Nishiyama, A., Mori, K. & Yodoi, J. (1997). AP-1 transcriptional activity is regulated by a direct association between thioredoxin and Ref-1. *Proc. Natl Acad. Sci. USA,* **94**, 3633-3638.
39. Qin, J., Clore, G. M., Kennedy, W. P., Kuszewski, J. & Gronenborn, A. M. (1996). The solution structure of human thioredoxin complexed with its target from Ref-1 reveals peptide chain reversal. *Structure,* **4**, 613-620.
40. Rothwell, D. G. & Hickson, I. D. (1996). Asparagine 212 is essential for abasic site recognition by the human DNA repair endonuclease HAP1. *Nucl. Acids Res.* **24**, 4217-4221.
41. Buckingham, D. A. & Engelhardt, L. M. (1975). Metal hydroxyl promoted hydrolysis of carbonyl substrates. *J. Am. Chem. Soc.* **97**, 5915-5917.
42. Masuda, Y., Bennett, R. A. O. & Demple, B. (1998). Dynamics of the interaction of human apurinic endonuclease (Ape1) with its substrate and product. *J. Biol. Chem.* **273**, 30352-30359.
43. Cowan, J. A. (1998). Metal activation of enzymes in nucleic acid biochemistry. *Chem. Rev.* **98**, 1067-1087.
44. Kalnick, M. W., Chang, C. N., Johnson, F., Grollman, A. P. & Patel, D. J. (1989). NMR studies of abasic sites in DNA duplexes: deoxyadenosine stacks into the helix opposite abasic lesions. *Biochemistry,* **28**, 3373-3383.
45. Izumi, T., Malecki, J., Chaudhry, M. A., Weinfeld, M., Hill, J. H., Lee, J. C. & Mitra, S. (1999). Intragenic suppression of an active site mutation in the human apurinic/apyrimidinic endonuclease. *J. Mol. Biol.* **287**, 47-57.
46. Jones, S. J., Worrall, A. F. & Connolly, B. A. (1996). Site-directed mutagenesis of the catalytic residues of bovine pancreatic deoxyribonuclease I. *J. Mol. Biol.* **264**, 1154-1163.
47. Casareno, R. L. B. & Cowan, J. A. (1996). Magnesium vs. manganese cofactors for metallonuclease enzymes. A critical evaluation of thermodynamic binding parameters and stoichiometry. *Chem. Commun.* **1996**, 1813-1814.
48. Leslie, A. G. W. (1992). *CPCr and ESF-EACMB Newsletter on Protein Crystallography,* no. 26, Daresbury, UK.
49. Collaborative Computational Project Number 4 (1994). The CCP4 suite: programs for protein crystallography. *Acta Crystallog. sect. D,* **50**, 760-763.
50. Kissinger, C. R., Gehlhaar, D. K. & Fogel, D. B. (1999). Rapid automated molecular replacement by evolutionary search. *Acta Crystallog. sect. D,* **55**, 484-491.
51. Segelke, B. W., Forstner, M., Knapp, M., Trakhanov, S. D., Parkin, S. & Newhouse, Y. M. *et al*. (2000). Conformational flexibility in the apolipoprotein E amino-terminal domain structure determined from three new crystal forms: implications for lipid binding. *Protein Sci.* **9**, 886-897.
52. Perrakis, A., Sixma, T. K., Wilson, K. S. & Lamzin, V. S. (1997). wARP: improvement and extension of crystallographic phases by weighted averaging of multiple refined dummy atomic models. *Acta Crystallog. sect. D,* **53**, 448-455.
53. Tronrud, D. E., Ten, Eyck L. F. & Matthews, B. W. (1987). An efficient general-purpose least-squares refinement program for macromolecular structures. *Acta Crystallog. sect. A,* **43**, 489-501.
54. Lamzin, V. S. & Wilson, K. S. (1997). Automated refinement for protein crystallography. *Methods Enzymol.* **277**, 269-305.
55. Hooft, R. W. W., Vriend, G., Sander, C. & Abola, E. E. (1996). Errors in protein structures. *Nature,* **381**, 272.

Edited by I. A. Wilson

(Received 15 November 2000; received in revised form 26 January 2001; accepted 26 January 2001)